Hindawi
Mathematical Problems in Engineering
Volume 2018, Article ID 1934174, 11 pages
https://doi.org/10.1155/2018/1934174

Research Article

Dual Number-Based Relative Position and Attitude Coordinated Control for Multi-Rigid-Body System

Jing Li

School of Medical Information Engineering, Jining Medical University, Rizhao 276826, China

Correspondence should be addressed to Jing Li; ning20140822@126.com

Received 21 March 2018; Revised 26 September 2018; Accepted 4 October 2018; Published 25 November 2018

Academic Editor: Jean Jacques Loiseau

The paper focuses on finding a dual number solution to position and attitude coordinated control for a multi-rigid-body system. First, a relative motion coupling model of a multi-rigid-body system is established under the framework of dual number and dual quaternion theory. Then, a coordinated control strategy that uses graph theory based on a derived new type of dual quaternion is proposed to simultaneously control the position and attitude of a multi-rigid-body system. Finally, the resulting Lyapunov function is proved to be almost globally asymptotically stable. The simulation results show that the proposed algorithm not only achieves unified control of position and attitude but also exhibits better tracking control performance.

1. Introduction

Multiagent systems have become an important topic of research in recent years, with an increasing number of scholars researching them. The object of this research is a set of self-governing agent groups in which multiple agents exchange information such as goals, strategies, and plans. Compared with a single subsystem, a multiagent system is more robust. A multibody system is a special type of multiagent system that not only has the advantages of a multiagent system but is also widely used in the fields of unmanned aerial vehicle (UAV) cooperation tracking, satellite formation flights, intelligent transportation, distributed sensor networks, and swarm robot systems, which are all of increasing interest to researchers. Formation control, as an important research direction of the coordinated control of multi-rigid-body systems, has become a pressing issue in the field of control research in recent years [1–17]. For example, regarding the research of networks [1–4], the authors of [1] investigated the controllability issues of multiagent networks and then proposed a new perspective to graphical characterization of multiagent controllability [2]; the author of [3] investigated the bipartite consensus problem for multiagent systems with second-order dynamics and antagonistic interactions; and in [4], the output feedback control and stabilization of multiplicative noise systems with intermittent observations were proposed. Regarding the research of spacecraft formation [5–10], the authors of [6] proposed a decentralized coordinated attitude control law for satellite formation flying, while the authors of [8] proposed a relative orbit estimation and formation to maintain control of satellite formations in low Earth orbits; and in [9], the authors considered a distributed attitude alignment problem for a team of deep-space formation flying spacecraft with the assistance of local information exchanges. Regarding the research of unmanned aerial vehicle formations [11, 12], the authors of [11] proposed a distributed output feedback formation tracking control law for UAVs, and in [12], a distributed UAV formation control method using a differential game approach was proposed. In research on multirobot formation [13, 14], the authors of [13] designed and implemented a novel decentralized control scheme that achieves dynamic formation control and collision avoidance for a group of nonholonomic robots, and in [14], a novel cooperative coevolutionary algorithm was proposed. However, the abovementioned algorithms consider relative motion control of the position and attitude of a multi-rigid-body formation as two separate subsystems. As an alternative solution, some scholars have proposed an integrated coupling of position and attitude dynamic models and control methods [15–17]. For example, the

authors of [15] proposed a six-degree-of-freedom spacecraft formation control method with possible switching topology. By rearranging the combined translational and rotational dynamics into a unified Euler-Lagrange formulation, the developed controllers can be applied directly to maintain formation and desired relative attitudes. The authors of [16] established a six-degree-of-freedom model of the satellite's orbit and attitude coupling based on master-slave structure and constructed an output feedback control strategy without measuring the angular velocity. Although this algorithm treats the characteristics of position and attitude as if they were coupled, it is still based on separate descriptions of position and attitude, and thus, two sets of control laws still need to be designed, thereby increasing the computational complexity.

As a basic problem of the coordinated control of a multiagent system, the problem of consistency had been a matter of concern for an increasing number of researchers [18–24]. In [18], the leader-following consensus problem of higher-order multiagent systems is considered; in [19], a network-based consensus control protocol under a directed graph is proposed; and in [20], a robust adaptive control approach for solving the consensus problem of multiagent systems is proposed. A multi-rigid-body system is a special type of multiagent system, and formation control is an important problem that is closely related to the problem of consistency in the coordinated control of multi-rigid-body systems. At present, in the context of the coordinated control of a multi-rigid-body formation, most scholars still do not consider the problem of information interaction between rigid bodies and thus cannot coordinate rigid body formation.

To offer a solution for the outlined problems, this paper proposes a distributed coordinated control algorithm of multi-rigid-body systems based on dual number theory and graph theory. The rest of the paper is organized as follows. Section 2 introduces the concepts of dual number and dual vector along with graph theory. Then, the relative dynamics models for a multi-rigid-body within the dual quaternion theory framework are derived. In the next section, according to the quaternion logarithm operation and the dual quaternion Lie group properties, we define a new dual quaternion, $\widehat{\mathbf{Q}}$, and on the basis of the new dual quaternion, a coordinated control law is deduced. Then, the control law is proved to be almost globally asymptotically stable. Finally, a numerical example is used to verify the effectiveness of the proposed control law.

2. Related Concepts

2.1. Dual Number. The concept of dual number was first proposed by Clifford as follows [25]:

$$\widehat{z} = z + \varepsilon z' \tag{1}$$

where z is the real part of the dual number, z' is the dual part, and ε is the dual unit, which satisfies $\varepsilon^2 = 0$.

A dual vector is a special type of dual number that has real and dual parts that are vectors. For example, the dual vector $\widehat{\boldsymbol{F}}$, which is composed of the force $\boldsymbol{f}$ acting on a rigid body and the produced torque $\boldsymbol{\tau}$ relative to point O, is

$$\widehat{\boldsymbol{F}} = \boldsymbol{f} + \varepsilon\boldsymbol{\tau} \tag{2}$$

While the torque acting on a rigid body depends on the choice of a reference point, the force does not depend on a reference point.

If the angular velocity of a rigid body at a certain time is $\boldsymbol{\omega}$, and the velocity at a point O is $\boldsymbol{v}$, then the dual vector $\widehat{\boldsymbol{\omega}}$ can be expressed as follows:

$$\widehat{\boldsymbol{\omega}} = \boldsymbol{\omega} + \varepsilon\boldsymbol{v} \tag{3}$$

A dual quaternion can be described as a dual number whose real and dual parts are both unit quaternions, as defined by

$$\widehat{\boldsymbol{q}} = \boldsymbol{q}_r + \varepsilon\boldsymbol{q}_d \tag{4}$$

In (4), the real part $\boldsymbol{q}_r$ and the dual part $\boldsymbol{q}_d$ are both quaternion; the real part describes the rotation of the rigid body, and the dual part describes its translation.

Quaternions and dual quaternions have similar properties:

$$\begin{aligned}
&\textit{Addition}: \widehat{\boldsymbol{a}} \pm \widehat{\boldsymbol{b}} = (\boldsymbol{a}_r \pm \boldsymbol{b}_r) + \varepsilon(\boldsymbol{a}_d \pm \boldsymbol{b}_d)\\
&\textit{Multiplication}: \widehat{\boldsymbol{a}} \circ \widehat{\boldsymbol{b}}\\
&\quad = (\boldsymbol{a}_r \circ \boldsymbol{b}_r) + \varepsilon(\boldsymbol{a}_r \circ \boldsymbol{b}_d + \boldsymbol{a}_d \circ \boldsymbol{b}_r)\\
&\textit{Conjugate}: \widehat{\boldsymbol{a}}^* = \boldsymbol{a}_r{}^* + \varepsilon\boldsymbol{a}_d^*\\
&\textit{Exchange}: \widehat{\boldsymbol{a}}^s = \boldsymbol{a}_d + \varepsilon\boldsymbol{a}_r\\
&\textit{Scalar part}: (\widehat{\boldsymbol{a}})_s = (\boldsymbol{a}_r)_s + \varepsilon(\boldsymbol{a}_d)_s\\
&\textit{Vector part}: (\widehat{\boldsymbol{a}})_v = (\boldsymbol{a}_r)_v + \varepsilon(\boldsymbol{a}_d)_v
\end{aligned} \tag{5}$$

From the basic properties of the dual quaternions, the following conclusion can be drawn:

$$\widehat{\boldsymbol{a}} \cdot (\widehat{\boldsymbol{b}} \circ \widehat{\boldsymbol{c}}) = \widehat{\boldsymbol{b}}^s \cdot (\widehat{\boldsymbol{a}}^s \circ \widehat{\boldsymbol{c}}^*) = \widehat{\boldsymbol{c}}^s \cdot (\widehat{\boldsymbol{b}}^* \circ \widehat{\boldsymbol{a}}^s) \tag{6}$$

If $\widehat{\boldsymbol{q}} \circ \widehat{\boldsymbol{q}}^* = \widehat{\mathbf{1}} = [0,0,0,1]^{\mathrm{T}} + \varepsilon[0,0,0,1]^{\mathrm{T}}$, then the dual quaternion $\widehat{\boldsymbol{q}}$ is called a unit dual quaternion.

2.2. Graph Theory. Multi-rigid-body systems are essentially a class of multiagent systems, and each rigid-body is considered an individual component in a multiagent system. Each individual component acquires its own control laws through interaction with its neighbours and thereby realizes overall control. In this paper, the topology of the multi-rigid-body system is modelled by graph theory.

Directed and undirected graphs are the most suitable mathematical objects for modelling the information topology of communications and perceptions between multiple rigid bodies. The directed graph is denoted by $G = (V, E)$ and consists of a set of nonempty nodes $V = \{1, \ldots, n\}$ representing the rigid bodies and a set of edges E representing

the relationships between communications and perceptions. When $E = \mathrm{diag}(a_1, \ldots, a_m)$, the matrix has full rank. The adjacency matrix of graph G is defined as $\boldsymbol{A} \triangleq [a_{ij}] \in R^{n\times n}$, and the weights a_{ij} satisfy $a_{ij} > 0$ when $(i, j) \in E$ and $a_{ij} = 0$ otherwise. In an undirected graph, $a_{ij} = a_{ji}, \forall i, j \in V$.

The interaction between individual agents is realized through the following protocol [26]:

$$y_i = -\sum_{j=1}^{n} a_{ij}\left[\left(x_i - x_j\right)\right] \tag{7}$$

where the indices i and j specify a given rigid body in the topological network.

3. Multi-Rigid-Body System Relative Kinematics and Dynamics Model

The rigid-body kinematics are given by

$$\begin{aligned} \dot{\hat{\boldsymbol{q}}}_i &= \frac{1}{2}\hat{\boldsymbol{q}}_i \circ \widehat{\boldsymbol{\omega}}_i \\ \widehat{\boldsymbol{\omega}}_i &= \boldsymbol{\omega}_i + \varepsilon\left(\dot{\mathbf{r}}_i + \boldsymbol{\omega}_i \times \mathbf{r}_i\right) \\ & \qquad i = 1, \ldots, n \end{aligned} \tag{8}$$

where n is the total number of rigid bodies in the team.

The relative kinematics equation of the multi-rigid-body system, written in terms of dual numbers, is

$$\hat{\boldsymbol{q}}_{ij} = \hat{\boldsymbol{q}}_j^* \circ \hat{\boldsymbol{q}}_i = \boldsymbol{q}_{ij} + \varepsilon\frac{1}{2}\boldsymbol{r}_{ij} \circ \boldsymbol{q}_{ij} \tag{9}$$

where i and j represent the ith and jth rigid body, respectively, and $\hat{\boldsymbol{q}}_{ij}$ is the dual quaternion of the ith rigid body relative to the jth rigid body. From $\hat{\boldsymbol{q}}_{ij}$, one can calculate the relative position and attitude between two rigid bodies. $\boldsymbol{q}_{ij}$ is the attitude quaternion of the ith rigid body relative to the jth rigid body, and $\boldsymbol{q}_{ij} = \boldsymbol{q}_j^* \circ \boldsymbol{q}_i$. $\boldsymbol{r}_{ij}$ is the absolute value of the relative position vector in the ith rigid body frame.

Theorem 1. *For the ith and jth rigid bodies, the relative dynamics equation can be derived as* $\dot{\widehat{\boldsymbol{\omega}}}_{ij} + \widehat{\mathbf{M}}_j^{-1}(\widehat{\boldsymbol{\omega}}_j \times \widehat{\mathbf{M}}_j\widehat{\boldsymbol{\omega}}_j) + \hat{\boldsymbol{q}}_{ij}^* \circ \dot{\widehat{\boldsymbol{\omega}}}_i \circ \hat{\boldsymbol{q}}_{ij} - \widehat{\boldsymbol{\omega}}_{ij} \times (\hat{\boldsymbol{q}}_{ij}^* \circ \widehat{\boldsymbol{\omega}}_i \circ \hat{\boldsymbol{q}}_{ij}) = \widehat{\mathbf{M}}_j^{-1}\hat{\boldsymbol{F}}_j$, *where* $\widehat{\mathbf{M}}_j$ *is the dual inertia matrix of the jth rigid body, and* $\hat{\boldsymbol{F}}_j$ *is the dual force acting on the jth rigid body.*

Proof. The dual velocity can be written as

$$\widehat{\boldsymbol{\omega}}_{ij} = \widehat{\boldsymbol{\omega}}_j - \hat{\boldsymbol{q}}_{ij}^* \circ \widehat{\boldsymbol{\omega}}_i \circ \hat{\boldsymbol{q}}_{ij} \tag{10}$$

where $\widehat{\boldsymbol{\omega}}_{ij}$ is the dual velocity of the ith rigid body relative to the jth rigid body, $\widehat{\boldsymbol{\omega}}_i$ is expressed in i-frame coordinates, and $\widehat{\boldsymbol{\omega}}_j$ is expressed in j-frame coordinates; they are dual velocities relative to the inertial frame. $\hat{\boldsymbol{q}}_{ij}^*$ is the conjugate of $\hat{\boldsymbol{q}}_{ij}$.

After taking the derivatives of formula (10) variables, we obtain formula (11):

$$\begin{aligned} \dot{\widehat{\boldsymbol{\omega}}}_{ij} &= \dot{\widehat{\boldsymbol{\omega}}}_j - \left(\hat{\boldsymbol{q}}_{ij}^* \circ \widehat{\boldsymbol{\omega}}_i \circ \hat{\boldsymbol{q}}_{ij}\right)' \\ &= \dot{\widehat{\boldsymbol{\omega}}}_j - \dot{\hat{\boldsymbol{q}}}_{ij}^* \circ \widehat{\boldsymbol{\omega}}_i \circ \hat{\boldsymbol{q}}_{ij} - \hat{\boldsymbol{q}}_{ij}^* \circ \dot{\widehat{\boldsymbol{\omega}}}_i \circ \hat{\boldsymbol{q}}_{ij} - \hat{\boldsymbol{q}}_{ij}^* \circ \widehat{\boldsymbol{\omega}}_i \circ \dot{\hat{\boldsymbol{q}}}_{ij} \\ &= \dot{\widehat{\boldsymbol{\omega}}}_j - \hat{\boldsymbol{q}}_{ij}^* \circ \dot{\widehat{\boldsymbol{\omega}}}_i \circ \hat{\boldsymbol{q}}_{ij} + \widehat{\boldsymbol{\omega}}_j \times \left(\hat{\boldsymbol{q}}_{ij}^* \circ \widehat{\boldsymbol{\omega}}_i \circ \hat{\boldsymbol{q}}_{ij}\right) \end{aligned} \tag{11}$$

The position and attitude coupling dynamic model of the ith and jth rigid body in the inertial frame are

$$\begin{aligned} \widehat{M}_i\dot{\widehat{\boldsymbol{\omega}}}_i + \boldsymbol{\omega}_i \times \widehat{M}_i\widehat{\boldsymbol{\omega}}_i &= \hat{\boldsymbol{F}}_i \\ \widehat{M}_j\dot{\widehat{\boldsymbol{\omega}}}_j + \widehat{\boldsymbol{\omega}}_j \times \widehat{M}_j\widehat{\boldsymbol{\omega}}_j &= \hat{\boldsymbol{F}}_j \end{aligned} \tag{12}$$

where the dual matrix of the inertia of the rigid body is given in [27]

$$\widehat{\boldsymbol{M}} = \widehat{\boldsymbol{m}} + \hat{\boldsymbol{J}} = m\frac{d}{d\varepsilon}\boldsymbol{I}_{3\times 3} + \varepsilon\boldsymbol{J} \tag{13}$$

In this formula, $\widehat{\boldsymbol{m}}$ is the mass of the follower rigid body, $\boldsymbol{I}_{3\times 3}$ is the third-order unit matrix, and $\boldsymbol{J}$ is the rotational inertia of the follower rigid body. The inverse $\widehat{\boldsymbol{M}}^{-1}$ of dual inertia matrix $\widehat{\boldsymbol{M}}$ is defined as follows:

$$\widehat{\boldsymbol{M}}^{-1} = \boldsymbol{J}^{-1}\frac{d}{d\varepsilon} + \varepsilon\left(\frac{1}{m}\right)\boldsymbol{I} \tag{14}$$

The following expression can be obtained from formula (12):

$$\begin{aligned} \dot{\widehat{\boldsymbol{\omega}}}_i &= -\widehat{\boldsymbol{M}}_i^{-1}\left(\widehat{\boldsymbol{\omega}}_i \times \widehat{\boldsymbol{M}}_i\widehat{\boldsymbol{\omega}}_i\right) + \widehat{\boldsymbol{M}}_i^{-1}\hat{\boldsymbol{F}} \\ \dot{\widehat{\boldsymbol{\omega}}}_j &= -\widehat{\boldsymbol{M}}_j^{-1}\left(\widehat{\boldsymbol{\omega}}_j \times \widehat{\boldsymbol{M}}_j\widehat{\boldsymbol{\omega}}_j\right) + \widehat{\boldsymbol{M}}_j^{-1}\hat{\boldsymbol{F}} \end{aligned} \tag{15}$$

Substituting formula (15) into formula (11), we can obtain formula (16):

$$\begin{aligned} \dot{\widehat{\boldsymbol{\omega}}}_{ij} + \widehat{\mathbf{M}}_j^{-1}\left(\widehat{\boldsymbol{\omega}}_j \times \widehat{\mathbf{M}}_j\widehat{\boldsymbol{\omega}}_j\right) + \hat{\boldsymbol{q}}_{ij}^* \circ \dot{\widehat{\boldsymbol{\omega}}}_i \circ \hat{\boldsymbol{q}}_{ij} - \widehat{\boldsymbol{\omega}}_{ij} \\ \times \left(\hat{\boldsymbol{q}}_{ij}^* \circ \widehat{\boldsymbol{\omega}}_i \circ \hat{\boldsymbol{q}}_{ij}\right) = \widehat{\mathbf{M}}_j^{-1}\hat{\boldsymbol{F}}_j \end{aligned} \tag{16}$$

Formula (16) is the relative dynamics equation.
Hence, we complete the proof. □

4. Design of the Coordinated Control Law

4.1. Design of a New Dual Quaternion. According to the Euler theorem, the attitude of one coordinate system relative to the other can be obtained by rotating the angle φ around the unit axis $\mathbf{n}$; then, the unit quaternion can be expressed as

$$\boldsymbol{q} = \left(\cos\frac{\varphi}{2}, \sin\frac{\varphi}{2}\mathbf{n}\right) \tag{17}$$

Lemma 2. *The logarithmic mapping of a unit dual quaternion can be written as*

$$\widehat{\mathbf{Q}}_{ij} = \ln\hat{\boldsymbol{q}}_{ij} = \boldsymbol{q}_{ij} + \varepsilon\frac{1}{2}\boldsymbol{r}_{ij} \tag{18}$$

Proof. Using the quaternion logarithm and the dual quaternion Lie group properties [28], we arrive at the following formula:

$$\begin{aligned}\ln \widehat{\boldsymbol{q}}_{ij} &= \ln\left(\boldsymbol{q}_{ij} \circ e^{\varepsilon \boldsymbol{q}_{ij}^{-1} \circ \boldsymbol{q}_{ijd}}\right) = \ln\left(\boldsymbol{q}_{ij}\right) + \varepsilon \boldsymbol{q}_{ij}^{-1} \circ \boldsymbol{q}_{ijd} \\ &= \frac{1}{2}\left(\varphi \mathbf{n} + \varepsilon \boldsymbol{r}_{ij}\right)\end{aligned} \tag{19}$$

When φ is small,

$$\frac{1}{2}\left(\varphi \mathbf{n} + \varepsilon \boldsymbol{r}_{ij}\right) \approx \frac{1}{2}\mathbf{n}\sin\varphi + \varepsilon\frac{1}{2}\boldsymbol{r}_{ij} = \boldsymbol{q}_{ij} + \varepsilon\frac{1}{2}\boldsymbol{r}_{ij} \tag{20}$$

The real and dual parts of the logarithmic dual quaternion correspond exactly to position and attitude. Therefore, we define a new dual quaternion as follows:

$$\widehat{\boldsymbol{Q}}_{ij} = \boldsymbol{q}_{ij} + \varepsilon\frac{1}{2}\boldsymbol{r}_{ij} \tag{21}$$

Hence, we complete the proof. □

4.2. Design of the Control Law. The design of a multi-rigid-body system coordination control law mainly solves the pose coordination problem. As long as all state variables are bounded, it is ensured that each rigid body tracks the desired pose. Suppose that two rigid bodies are represented by i and j; then, when $t \longrightarrow \infty$,

$$\begin{aligned}&\widehat{\boldsymbol{q}}_i(t) \longrightarrow \widehat{\boldsymbol{q}}_j(t) \longrightarrow \widehat{\boldsymbol{q}}_d(t) \\ &\widehat{\boldsymbol{\omega}}_i(t) \longrightarrow \widehat{\mathbf{0}}\end{aligned} \tag{22}$$

where $\widehat{\boldsymbol{q}}_d(t)$ is the expected value of the rigid body's relative position and attitude.

Theorem 3. *For the relative motion coupling model based on the dual quaternion (9) and (16), the control law is written as follows:*

$$\widehat{\boldsymbol{F}}_i = -\lambda_i^p \widehat{\boldsymbol{Q}}_{ei}^s - \lambda_i^d \widehat{\boldsymbol{\omega}}_i - \sum_{j=1}^{n} a_{ij}^p \widehat{\boldsymbol{Q}}_{ij}^s \tag{23}$$

Proof. The ideal position and attitude coordinated control law is designed as follows:

$$\widehat{\boldsymbol{F}}_i = \widehat{\boldsymbol{F}}_i^s + \widehat{\boldsymbol{F}}_i^f \tag{24}$$

where $\widehat{\boldsymbol{F}}_i^s$ is called the absolute pose tracking item and is used to track the overall desired position and attitude of the multi-rigid-body system; $\widehat{\boldsymbol{F}}_i^f$ is called the relative pose preservation item and is used to adjust the pose of the current rigid body (according to the pose of the adjacent rigid body) to ensure that the relative position and altitude of the multi-rigid-body remain consistent. According to the graph theory, the expressions for $\widehat{\boldsymbol{F}}_i^s$ and $\widehat{\boldsymbol{F}}_i^f$ are

$$\widehat{\boldsymbol{F}}_i^s = -\lambda_i^p \widehat{\boldsymbol{Q}}_{ei}^s - \lambda_i^d \widehat{\boldsymbol{\omega}}_i \tag{25}$$

$$\widehat{\boldsymbol{F}}_i^f = -\sum_{j=1}^{n} a_{ij}^p \widehat{\boldsymbol{Q}}_{ij}^s \tag{26}$$

where $\widehat{\boldsymbol{Q}}_{ei} = \widehat{\boldsymbol{Q}}_d^* \circ \widehat{\boldsymbol{Q}}_i = \boldsymbol{q}_{ei} + \varepsilon(1/2)\boldsymbol{r}_{ei}$ $\widehat{\boldsymbol{Q}}_{ij} = \widehat{\boldsymbol{Q}}_i^* \circ \widehat{\boldsymbol{Q}}_j = \boldsymbol{q}_{ij} + \varepsilon(1/2)\boldsymbol{r}_{ij}$, and λ_i^p and λ_i^d are positive constants. From formula (5), we obtain $\widehat{\boldsymbol{Q}}_{ei}^s = (\widehat{\boldsymbol{Q}}_d^* \circ \widehat{\boldsymbol{Q}}_i)^s = (1/2)\boldsymbol{r}_{ei} + \varepsilon \boldsymbol{q}_{ei}$ $\widehat{\boldsymbol{Q}}_{ij}^s = (\widehat{\boldsymbol{Q}}_i^* \circ \widehat{\boldsymbol{Q}}_j)^s = (1/2)\boldsymbol{r}_{ij} + \varepsilon \boldsymbol{q}_{ij}$. a_{ij}^p is the ith row and jth column element of the weighted adjacency matrix associated with the graph for the relative pose $\widehat{\boldsymbol{Q}}_{ij}^s$. □

4.3. Stability Analysis. We present the stability conclusions of the proposed multi-rigid-body system coordinated control algorithm in the form of a theorem.

Theorem 4. *Assume that the control law is given by formula (23) and the undirected communication graph is connected; then, the multi-rigid-body system can achieve pose tracking and effective pose coordination. When $t \longrightarrow \infty$, then $\boldsymbol{q}_i \longrightarrow \boldsymbol{q}_j \longrightarrow \boldsymbol{q}_d$, $\widehat{\boldsymbol{\omega}}_i \longrightarrow 0$, and $\boldsymbol{r}_i \longrightarrow \boldsymbol{r}_j \longrightarrow \boldsymbol{r}_d$ asymptotically, $\forall i \neq j$.*

Proof. Consider a Lyapunov function candidate:

$$\begin{aligned}V = {} & \lambda_i^p \sum_{i=1}^{n} \left\|\widehat{\boldsymbol{q}}_{ei} - \widehat{\mathbf{1}}\right\|^2 + \frac{1}{2}\sum_{i=1}^{n}\sum_{j=1}^{n} a_{ij}^p \left\|\widehat{\boldsymbol{q}}_{ij} - \widehat{\mathbf{1}}\right\|^2 \\ & + \frac{1}{2}\sum_{i=1}^{n} \widehat{\boldsymbol{\omega}}_i^s \left(\widehat{\boldsymbol{M}}_i \widehat{\boldsymbol{\omega}}_i\right)\end{aligned} \tag{27}$$

Since $\widehat{\boldsymbol{M}}_i$ is a positive definite matrix, the Lyapunov function satisfies $V \geq 0$ if and only if $\widehat{\boldsymbol{q}}_{ei} \longrightarrow \widehat{\mathbf{1}}, \widehat{\boldsymbol{q}}_{ij} \longrightarrow \widehat{\mathbf{1}}, \widehat{\boldsymbol{\omega}}_i \longrightarrow 0$; if $V = 0$, then the Lyapunov function V is positive and definite.

Lemma 5. *If $\boldsymbol{V}_q = \|\widehat{\boldsymbol{q}}_{ei} - \widehat{\mathbf{1}}\|^2$, then $\dot{\boldsymbol{V}}_q = \widehat{\boldsymbol{\omega}}_i^s \cdot \widehat{\boldsymbol{Q}}_{ei}^s$, where $\widehat{\boldsymbol{q}}_{ei} = \widehat{\boldsymbol{q}}_d^* \circ \widehat{\boldsymbol{q}}_i$.*

Proof. Suppose

$$\mathbf{A} = \left\|\widehat{\boldsymbol{q}}_{ei} - \widehat{\mathbf{1}}\right\|^2 = \left(\widehat{\boldsymbol{q}}_{ei} - \widehat{\mathbf{1}}\right) \cdot \left(\widehat{\boldsymbol{q}}_{ei} - \widehat{\mathbf{1}}\right) \tag{28}$$

Then

$$\begin{aligned}\dot{\mathbf{A}} &= \dot{\widehat{\boldsymbol{q}}}_{ei}\left(\widehat{\boldsymbol{q}}_{ei} - \widehat{\mathbf{1}}\right) + \left(\widehat{\boldsymbol{q}}_{ei} - \widehat{\mathbf{1}}\right)\dot{\widehat{\boldsymbol{q}}}_{ei} = 2\left(\widehat{\boldsymbol{q}}_{ei} - \widehat{\mathbf{1}}\right) \cdot \dot{\widehat{\boldsymbol{q}}}_{ei} \\ &= \left(\widehat{\boldsymbol{q}}_{ei} - \widehat{\mathbf{1}}\right) \cdot \left(\widehat{\boldsymbol{q}}_{ei} \circ \widehat{\boldsymbol{\omega}}_i\right) = \widehat{\boldsymbol{\omega}}_i^s \cdot \left[\widehat{\boldsymbol{q}}_{ei}^* \circ \left(\widehat{\boldsymbol{q}}_{ei} - \widehat{\mathbf{1}}\right)^s\right] \\ &= \widehat{\boldsymbol{\omega}}_i^s \cdot \left[\widehat{\boldsymbol{q}}_{ei}^* \circ \left(\widehat{\boldsymbol{q}}_{ei} - \widehat{\mathbf{1}}\right)^s\right]_v\end{aligned} \tag{29}$$

Then

$$\begin{aligned}\widehat{\boldsymbol{q}}_{ei}^* \circ \left(\widehat{\boldsymbol{q}}_{ei} - \widehat{\mathbf{1}}\right)^s &= \left[\boldsymbol{q}_{ei}^* + \varepsilon\frac{1}{2}\left(\boldsymbol{q}_{ei} \circ \boldsymbol{r}_{ei}\right)^*\right] \\ &\quad \circ \left[\left(\boldsymbol{q}_{ei} - \mathbf{1}\right) + \varepsilon\frac{1}{2}\boldsymbol{q}_{ei} \circ \boldsymbol{r}_{ei}\right]^s \\ &= \left[\boldsymbol{q}_{ei}^* + \varepsilon\frac{1}{2}\left(\boldsymbol{q}_{ei} \circ \boldsymbol{r}_{ei}\right)^*\right]_v \\ &\quad \circ \left[\frac{1}{2}\boldsymbol{q}_{ei} \circ \boldsymbol{r}_{ei} + \varepsilon\left(\boldsymbol{q}_{ei} - \mathbf{1}\right)\right]_v\end{aligned}$$

$$
\begin{aligned}
&= \left[\frac{1}{2}\boldsymbol{q}_{ei}^{\ *} \circ \boldsymbol{q}_{ei} \circ \boldsymbol{r}_{ei}\right]_v \\
&\quad + \left[\varepsilon \boldsymbol{q}_{ei}^{\ *} \circ \left(\boldsymbol{q}_{ei} - \mathbf{1}\right)\right]_v \\
&\quad + \left[\varepsilon \frac{1}{4}\left(\boldsymbol{q}_{ei} \circ \boldsymbol{r}_{ei}\right)^* \circ \left(\boldsymbol{q}_{ei} \circ \boldsymbol{r}_{ei}\right)\right]_v \\
&= \frac{1}{2}\boldsymbol{r}_{ei} + \varepsilon\left(\mathbf{1} - \boldsymbol{q}_{ei}^{\ *}\right) = \frac{1}{2}\boldsymbol{r}_{ei} + \varepsilon \boldsymbol{q}_{ei} \\
&= \widehat{\mathbf{Q}}_{ei}^{s}
\end{aligned} \tag{30}
$$

Substituting $\widehat{\mathbf{Q}}_{ei}^{s}$ into formula (29), we obtain the following formula:

$$
\dot{\mathbf{A}} = \widehat{\boldsymbol{\omega}}_i^s \cdot \widehat{\mathbf{Q}}_{ei}^{s} \tag{31}
$$

Hence, we complete the proof. □

Similarly, by taking the derivative of formula (27), we can arrive at

$$
\dot{V} = \lambda_i^p \sum_{i=1}^{n} \widehat{\boldsymbol{\omega}}_i^s \widehat{\mathbf{Q}}_{ei}^{s} + \frac{1}{2}\sum_{i=1}^{n}\sum_{j=1}^{n} a_{ij}^p \widehat{\boldsymbol{\omega}}_{ij}^s \widehat{\mathbf{Q}}_{ij}^{s} + \sum_{i=1}^{n} \widehat{\boldsymbol{\omega}}_i^s \left(\widehat{\boldsymbol{M}}_i \dot{\widehat{\boldsymbol{\omega}}}_i\right) \tag{32}
$$

where

$$
\begin{aligned}
\boldsymbol{B} &= \frac{1}{2}\sum_{i=1}^{n}\sum_{j=1}^{n} a_{ij}^p \left(\widehat{\boldsymbol{\omega}}_i - \widehat{\boldsymbol{\omega}}_j\right)^s \widehat{\mathbf{Q}}_{ij}^{s} \\
&= \frac{1}{2}\sum_{i=1}^{n} \widehat{\boldsymbol{\omega}}_i^s \sum_{j=1}^{n} a_{ij}^p \widehat{\mathbf{Q}}_{ij}^{s} - \frac{1}{2}\sum_{i=1}^{n} \widehat{\boldsymbol{\omega}}_j^s \sum_{j=1}^{n} a_{ij}^p \widehat{\mathbf{Q}}_{ij}^{s} \\
&= \frac{1}{2}\sum_{i=1}^{n} \widehat{\boldsymbol{\omega}}_i^s \sum_{j=1}^{n} a_{ij}^p \widehat{\mathbf{Q}}_{ij}^{s} + \frac{1}{2}\sum_{i=1}^{n} \widehat{\boldsymbol{\omega}}_j^s \sum_{j=1}^{n} a_{ji}^p \widehat{\mathbf{Q}}_{ji}^{s} \\
&= \sum_{i=1}^{n} \widehat{\boldsymbol{\omega}}_i^s \sum_{j=1}^{n} a_{ij}^p \widehat{\mathbf{Q}}_{ij}^{s}
\end{aligned} \tag{33}
$$

Then, formula (32) can be further simplified:

$$
\dot{V} = \sum_{i=1}^{n} \widehat{\boldsymbol{\omega}}_i^{\ s} \left[\lambda_i^p \widehat{\mathbf{Q}}_{ei}^{s} + \sum_{j=1}^{n} a_{ij}^p \widehat{\mathbf{Q}}_{ij}^{s} + \widehat{\mathbf{F}}_i - \left(\widehat{\boldsymbol{\omega}}_i \times \widehat{\mathbf{M}}_i \widehat{\boldsymbol{\omega}}_i\right)\right] \tag{34}
$$

Substituting the value of $\widehat{\mathbf{F}}_i$ into formula (34), we obtain

$$
\begin{aligned}
\dot{V} &= \sum_{i=1}^{n} \widehat{\boldsymbol{\omega}}_i^{\ s} \\
&\quad \cdot \left[\lambda_i^p \widehat{\mathbf{Q}}_{ei}^{s} + \sum_{j=1}^{n} a_{ij}^p \widehat{\mathbf{Q}}_{ij}^{s} - \lambda_i^p \widehat{\mathbf{Q}}_{ei}^{s} - \lambda_i^d \widehat{\boldsymbol{\omega}}_i - \sum_{j=1}^{n} a_{ij}^p \widehat{\mathbf{Q}}_{ij}^{s}\right] \\
&= -\sum_{i=1}^{n} \widehat{\boldsymbol{\omega}}_i^{\ s} \lambda_i^d \widehat{\boldsymbol{\omega}}_i \le 0
\end{aligned} \tag{35}
$$

To make $\dot{V} \equiv 0$, there must be a case where $\widehat{\boldsymbol{\omega}}_i \equiv 0$, and when $\widehat{\boldsymbol{\omega}}_i \equiv 0$, we can obtain the following formula:

$$
\lambda_i^p \widehat{\mathbf{Q}}_{ei}^{s} + \sum_{j=1}^{n} a_{ij}^p \widehat{\mathbf{Q}}_{ij}^{s} = \mathbf{0} \quad i = 1, 2 \ldots n \tag{36}
$$

Formula (36) can be written in two parts:

$$
\lambda_i^p \left(\boldsymbol{q}_{ei}\right)_v + a_{ij}^p \sum_{j=1}^{n} \left(\boldsymbol{q}_{ij}\right)_v = \mathbf{0} \tag{37}
$$

$$
\lambda_i^p \boldsymbol{r}_{ei} + a_{ij}^p \sum_{j=1}^{n} \boldsymbol{r}_{ij} = \mathbf{0} \tag{38}
$$

According to [9], formula (37) can be written as

$$
\left[\boldsymbol{P}(t) \otimes \boldsymbol{I}\right] \boldsymbol{q}_v = 0 \tag{39}
$$

where $\otimes$ is the Kronecker product, $\boldsymbol{I}$ is the identity matrix, $\widehat{\boldsymbol{q}}_v$ is a column vector stack composed of $(\boldsymbol{q}_d^{\ *} \circ \boldsymbol{q}_l)_v, l = 1, 2 \ldots n$, and $\boldsymbol{P}(t) = [p_{ij}(t)] \in \mathbf{R}^{n \times n}$, where $p_{ii}(t) = \lambda_i^p + \sum_{j=1}^{n} a_{ij}^p (\boldsymbol{q}_d^{\ *} \circ \boldsymbol{q}_j)_s$ and $p_{ij}(t) = -a_{ij}^p (\boldsymbol{q}_d^{\ *} \circ \boldsymbol{q}_i)_s$. Since $|(\boldsymbol{q}_d^{\ *} \circ \boldsymbol{q}_j)_s| \le 1$, we see that $\boldsymbol{P}(t)$ is strictly diagonally dominant, and the matrix has full rank. It can be seen that $(\boldsymbol{q}_d^{\ *} \circ \boldsymbol{q}_i)_v = 0$. By LaSalle's invariance principle, we arrive at the conclusion that when $\dot{V} \equiv 0$, the condition $\boldsymbol{q}_d^{\ *} \circ \boldsymbol{q}_i - \widehat{\mathbf{1}} \equiv 0$ is satisfied. Therefore, when $t \longrightarrow \infty$, the following holds: $\boldsymbol{q}_d^{\ *} \circ \boldsymbol{q}_i \longrightarrow 1$, $\widehat{\boldsymbol{\omega}}_i \longrightarrow 0$ asymptotically. Equivalently, we know that $\boldsymbol{q}_i \longrightarrow \boldsymbol{q}_j \longrightarrow \boldsymbol{q}_d, \forall i \ne j$. Similarly, using formula (38), we can conclude that when $t \longrightarrow \infty, \boldsymbol{r}_i - \boldsymbol{r}_d \longrightarrow 0, \boldsymbol{r}_i \longrightarrow \boldsymbol{r}_j \longrightarrow \boldsymbol{r}_d, \forall i \ne j$.

Hence, we complete the proof. □

5. Simulation and Discussion

Using the presented theoretical analysis, we apply the proposed algorithm to the coordinated control of formation rigid bodies. Taking the pose-coordinated control of six rigid bodies as an example, we verify the effectiveness of the control law. Each rigid body is regarded as a node, and the undirected graph is used to model the information flow between the rigid bodies. The interactions between the rigid bodies are shown in Figure 1.

The initial attitude and position of the rigid bodies are listed in Table 1. The initial dual angular velocities of the rigid bodies are $\widehat{\boldsymbol{\omega}}_i(0) = [0 \ \ 0 \ \ 0]^{\mathrm{T}}$, and the desired attitude and position are $\boldsymbol{q}_d = [1 \ \ 0 \ \ 0 \ \ 0]^{\mathrm{T}}$ and $\boldsymbol{r}_d = [0 \ \ 0 \ \ 0]^{\mathrm{T}}$, respectively. $\lambda_i^p = 1 \ \ \lambda_i^d = 2$, $a_{ij}^p = 0.1$, and the simulation time is $t = 500$s.

Figures 2 and 3 are attitude and angular velocity tracking curves, respectively, and Figures 4 and 5 are position and velocity tracking curves, respectively. The attitude and angular velocity tracking curves of Figures 2 and 3 show that the attitude and angular velocity of rigid bodies 1, 3, and 5 converge to zero within 40 seconds, thereby completing the attitude tracking. The position and velocity tracking curves of Figures 4 and 5 show that the convergence time of the position tracking curve is slower than that

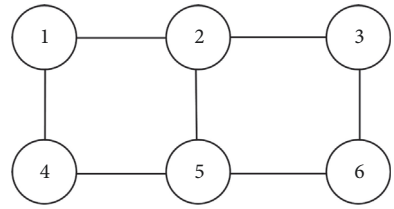

Figure 1: Undirected graph of rigid bodies.

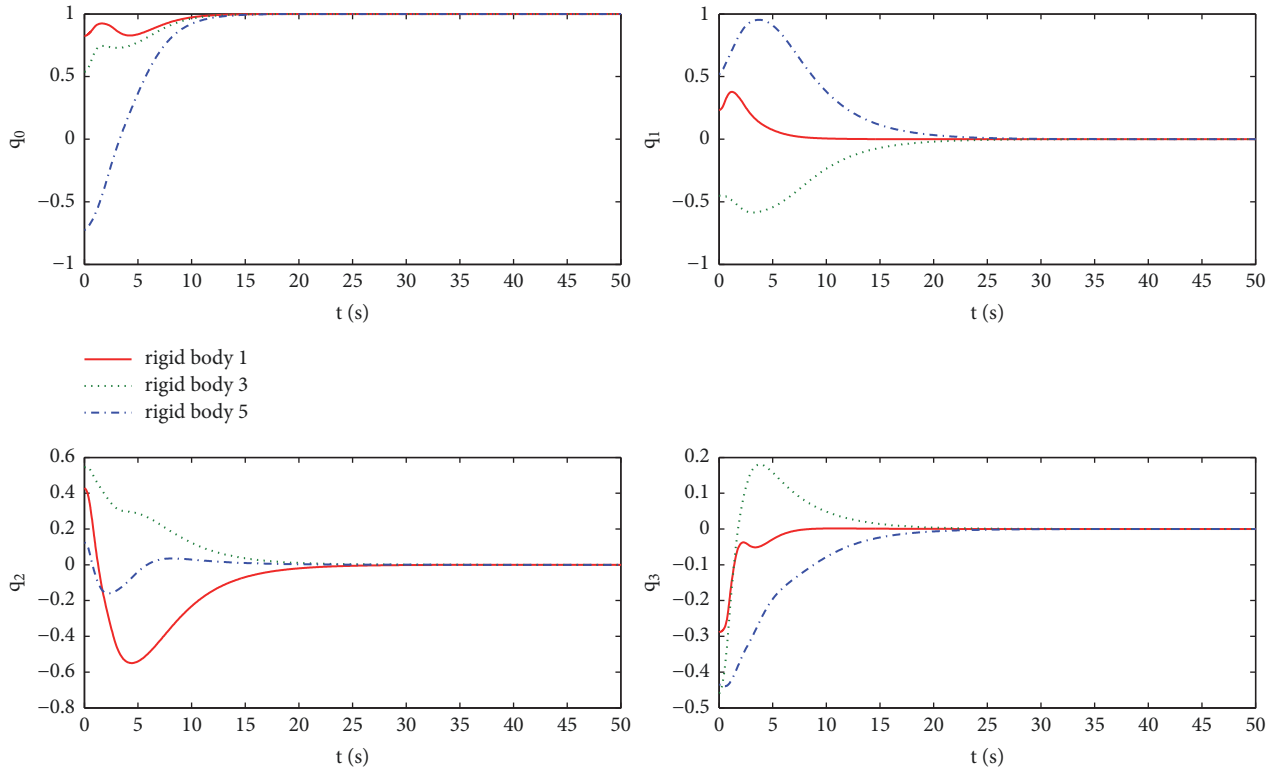

Figure 2: Attitude tracking curve.

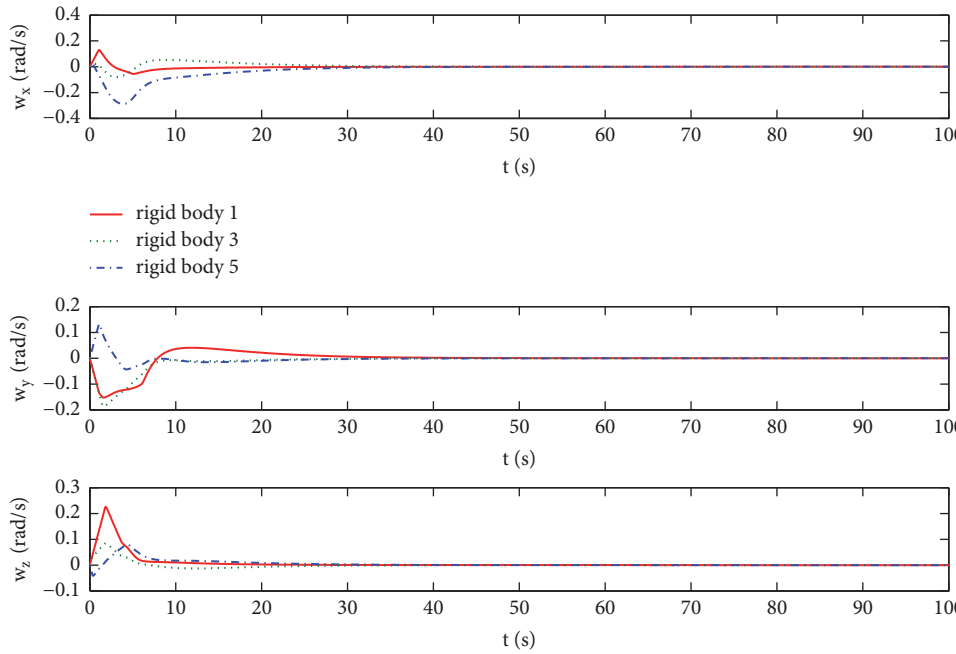

Figure 3: Angular velocity tracking curve.

Table 1: Initial attitude and position of the rigid bodies.

Rigid body	Initial attitude (q)	Initial position (m)
1	$[0.8243 \quad 0.2324 \quad 0.4283 \quad -0.2882]$	$[20 \quad 50 \quad 0]$
2	$[-0.9212 \quad -0.2468 \quad 0.2357 \quad 0.1869]$	$[20 \quad -50 \quad 0]$
3	$[0.5148 \quad -0.4302 \quad 0.5203 \quad -0.4389]$	$[-20 \quad 30 \quad 0]$
4	$[0.7028 \quad -0.4188 \quad 0.2176 \quad 0.5323]$	$[-20 \quad -30 \quad 0]$
5	$[-0.7238 \quad 0.5212 \quad 0.1235 \quad -0.4350]$	$[-40 \quad 20 \quad 0]$
6	$[0.3423 \quad 0.4215 \quad 0.6532 \quad -0.5277]$	$[-40 \quad -20 \quad 0]$

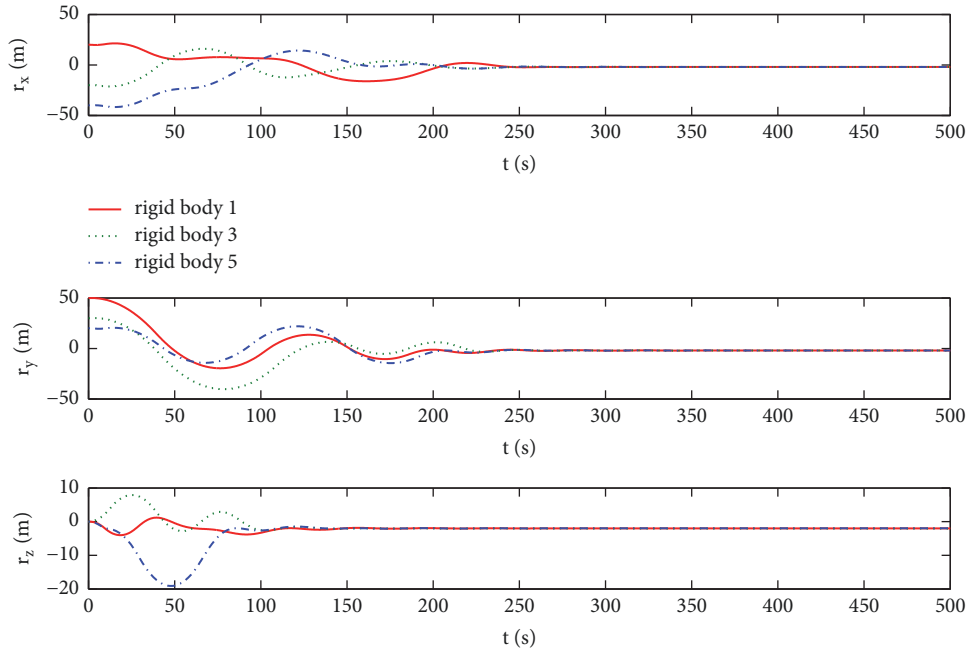

Figure 4: Position tracking curve.

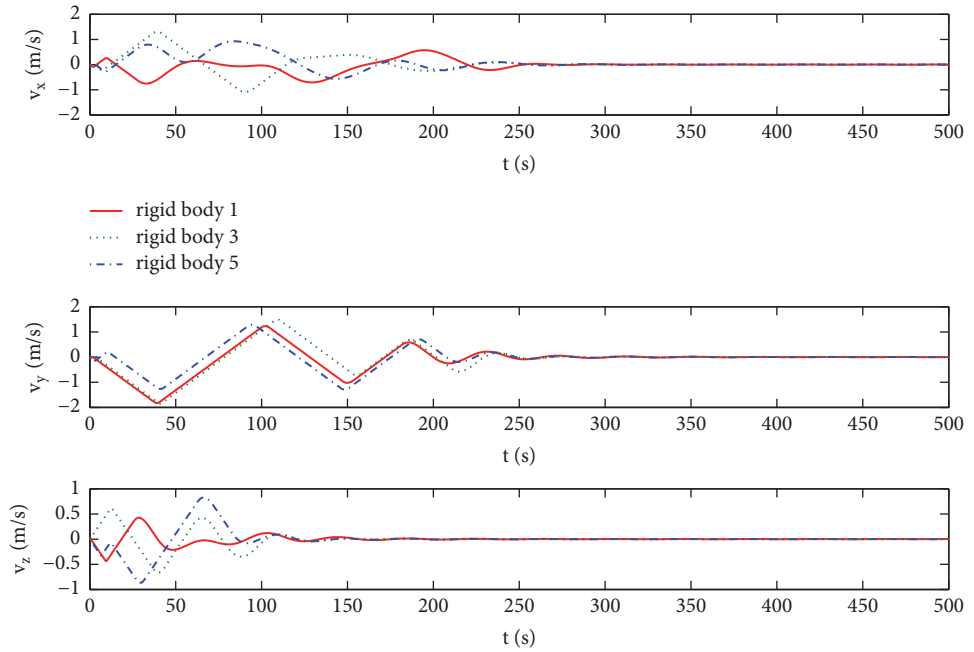

Figure 5: Velocity tracking curve.

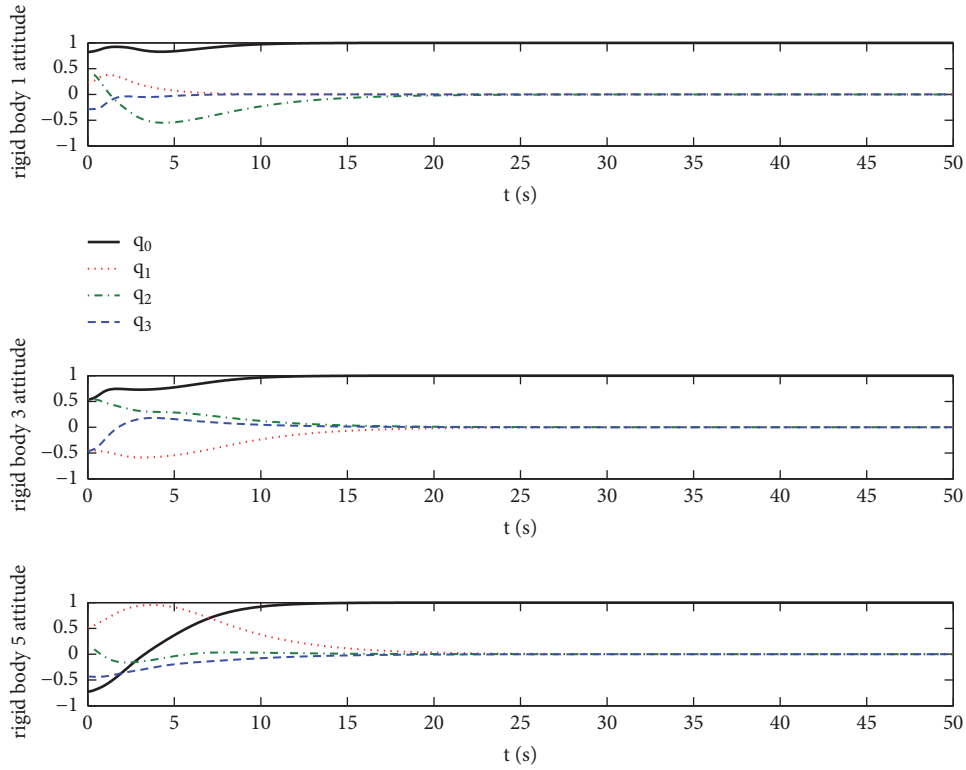

Figure 6: Attitude curves of rigid bodies 1, 3, and 5.

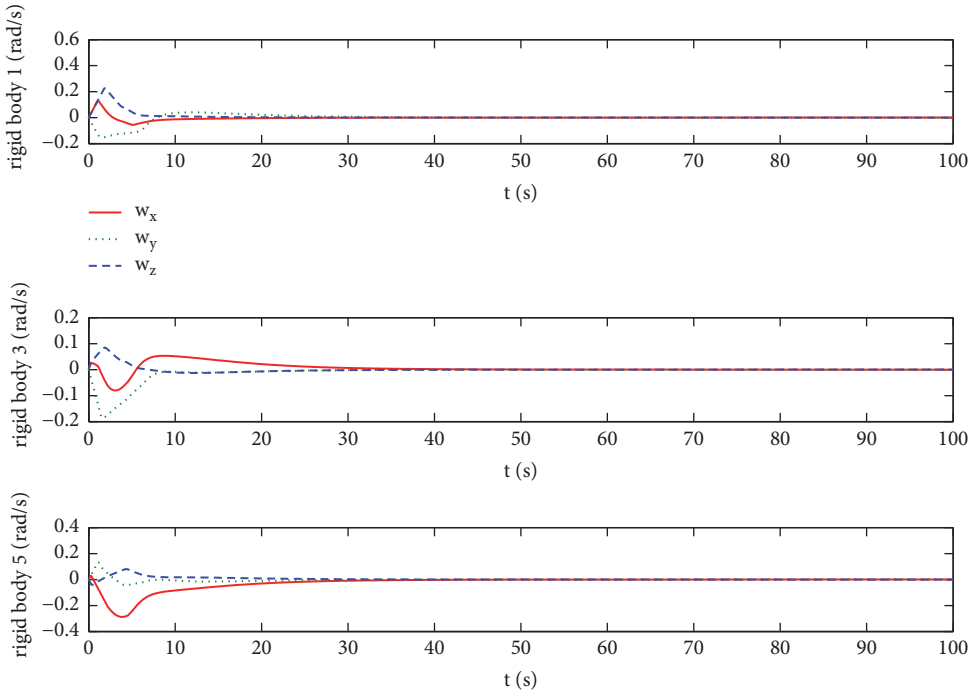

Figure 7: Angular velocity curves of rigid bodies 1, 3, and 5.

of the attitude tracking curve, and it converges to 0 in approximately 300 seconds. Thus, both the attitude and position tracking errors converge rapidly in a short period of time and satisfy the accuracy requirements. The multi-rigid-body system basically realizes attitude and position tracking.

To further demonstrate the effectiveness of the algorithm, we simulate the attitude, angular velocity, position, and velocity of each rigid body. The simulation results are shown in Figures 6, 7, 8 and 9.

Figures 6 and 7 are attitude and angular velocity tracking curves of rigid bodies 1, 3, and 5, respectively, and Figures

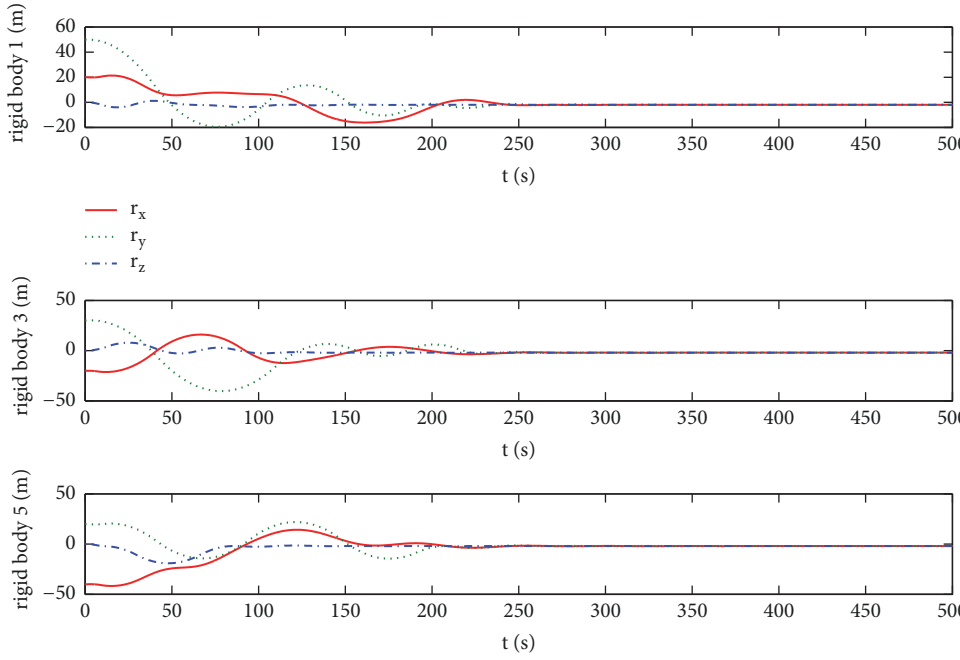

Figure 8: Position curves of rigid bodies 1, 3, and 5.

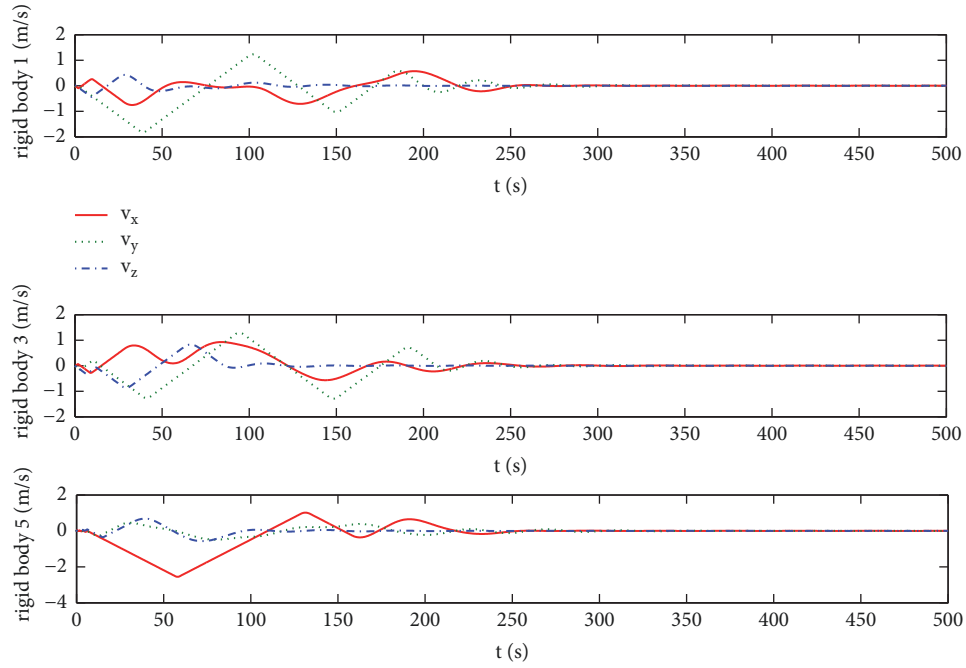

Figure 9: Velocity curves of rigid bodies 1, 3, and 5.

8 and 9 are position and velocity tracking curves of rigid bodies 1, 3, and 5, respectively. These figures show that both the attitude and position errors of every rigid body converge rapidly and satisfy the accuracy requirements despite the presence of the initial errors. Therefore, it is feasible to carry out position and attitude coordinated control of a multi-rigid-body system on the basis of dual number and dual quaternion. The simulation results show that the algorithm not only achieves unified control of relative position and attitude but also exhibits good tracking control performance.

6. Conclusions

A new type of dual quaternion is investigated in this study. From the derived form of dual quaternion together with graph theory, we proposed a novel coordinated control law

to simultaneously control position and attitude. Then, the Lyapunov function is used to prove that the model is almost globally asymptotically stable in terms of the control law. The simulation results indicate that the controller that considers the coupling effect performs better than the traditional controller that considers the relative position and attitude separately. Additionally, the proposed algorithm in this paper is simpler and can simultaneously control both relative position and attitude.

Data Availability

The data used to support the findings of this study are included within the article.

Conflicts of Interest

The author declares no conflicts of interest.

Acknowledgments

This work was supported by the Supporting Fund for Teachers' Research of Jining Medical University (No. JY2017KJ052).

References

[1] Z. Ji, H. Lin, and H. Yu, "Protocols design and uncontrollable topologies construction for multi-agent networks," *IEEE Transactions on Automatic Control*, vol. 60, no. 3, pp. 781–786, 2015.

[2] Z. Ji and H. Yu, "A new perspective to graphical characterization of multiagent controllability," *IEEE Transactions on Cybernetics*, vol. 47, no. 6, pp. 1471–1483, 2017.

[3] L. Tian, Z. Ji, T. Hou, and K. Liu, "Bipartite consensus on coopetition networks with time-varying delays," *IEEE Access*, vol. 6, pp. 10169–10178, 2018.

[4] Q. Qi and H. Zhang, "Output feedback control and stabilization for multiplicative noise systems with intermittent observations," *IEEE Transactions on Cybernetics*, 2017.

[5] P. P. Menon, C. Edwards, and N. M. Gomes Paulino, "Observer-based controller design with disturbance feedforward framework for formation control of satellites," *IET Control Theory & Applications*, vol. 9, no. 8, pp. 1285–1293, 2015.

[6] I. Chang, S.-Y. Park, and K.-H. Choi, "Decentralized coordinated attitude control for satellite formation flying via the state-dependent Riccati equation technique," *International Journal of Non-Linear Mechanics*, vol. 44, no. 8, pp. 891–904, 2009.

[7] Y. Wu, X. Cao, P. Zhang, and Z. Zeng, "Variable structure-based decentralized relative attitude-coordinated control for satellite formation," *IEEE Aerospace & Electronic Systems Magazine*, vol. 27, no. 12, pp. 18–25, 2012.

[8] G. Zeng, M. Ru, and R. Yao, "Relative orbit estimation and formation keeping control of satellite formations in low Earth orbits," *Acta Astronautica*, vol. 76, pp. 164–175, 2012.

[9] W. Ren, "Distributed attitude alignment in spacecraft formation flying," *International Journal of Adaptive Control and Signal Processing*, vol. 21, no. 2-3, pp. 95–113, 2007.

[10] H. Yang, X. You, and C. Hua, "Attitude tracking control for spacecraft formation with time-varying delays and switching topology," *Acta Astronautica*, vol. 126, pp. 98–108, 2016.

[11] L. He, X. Sun, and Y. Lin, "Distributed output-feedback formation tracking control for unmanned aerial vehicles," *International Journal of Systems Science*, vol. 47, no. 16, pp. 3919–3928, 2016.

[12] W. Lin, "Distributed UAV formation control using differential game approach," *Aerospace Science and Technology*, vol. 35, no. 1, pp. 54–62, 2014.

[13] S. Mastellone, D. M. Stipanović, C. R. Graunke, K. A. Intlekofer, and M. W. Spong, "Formation control and collision avoidance for multi-agent non-holonomic systems: Theory and experiments," *International Journal of Robotics Research*, vol. 27, no. 1, pp. 107–126, 2008.

[14] S.-M. Lee, H. Kim, H. Myung, and X. Yao, "Cooperative coevolutionary algorithm-based model predictive control guaranteeing stability of multirobot formation," *IEEE Transactions on Control Systems Technology*, vol. 23, no. 1, pp. 37–51, 2015.

[15] H. Min, S. Wang, F. Sun, Z. Gao, and Y. Wang, "Distributed six degree-of-freedom spacecraft formation control with possible switching topology," *IET Control Theory & Applications*, vol. 5, no. 9, pp. 1120–1130, 2011.

[16] J. Shan, "Synchronized attitude and translational motion control for spacecraft formation flying," *Proceedings of the Institution of Mechanical Engineers, Part G: Journal of Aerospace Engineering*, vol. 223, no. 6, pp. 749–768, 2009.

[17] S. Segal and P. Gurfil, "Effect of kinematic rotation-translation coupling on relative spacecraft translational dynamics," *Journal of Guidance, Control, and Dynamics*, vol. 32, no. 3, pp. 1045–1050, 2009.

[18] H. Hermansyah, A. Wijanarko, M. Kubo, N. Shibasaki-Kitakawa, and T. Yonemoto, "Leader-following consensus of multi-agent systems under fixed and switching topologies," *Systems & Control Letters*, vol. 59, no. 3-4, pp. 209–217, 2010.

[19] L. Ding, Q.-L. Han, and G. Guo, "Network-based leader-following consensus for distributed multi-agent systems," *Automatica*, vol. 49, no. 7, pp. 2281–2286, 2013.

[20] Z. G. Hou, L. Cheng, and M. Tan, "Decentralized robust adaptive control for the multiagent system consensus problem using neural networks," *IEEE Transactions on Systems, Man, and Cybernetics, Part B: Cybernetics*, vol. 39, no. 3, pp. 636–647, 2009.

[21] H. Geng, Z.-Q. Chen, Z.-X. Liu, and Q. Zhang, "Consensus of a heterogeneous multi-agent system with input saturation," *Neurocomputing*, vol. 166, pp. 382–388, 2015.

[22] J. Bai, G. Wen, A. Rahmani, X. Chu, and Y. Yu, "Consensus with a reference state for fractional-order multi-agent systems," *International Journal of Systems Science*, vol. 47, no. 1, pp. 222–234, 2016.

[23] Y. Zheng, Y. Zhu, and L. Wang, "Consensus of heterogeneous multi-agent systems," *IET Control Theory & Applications*, vol. 5, no. 16, pp. 1881–1888, 2011.

[24] G.-S. Han, Z.-H. Guan, J. Li, D.-X. He, and D.-F. Zheng, "Multi-tracking of second-order multi-agent systems using impulsive control," *Nonlinear Dynamics*, vol. 84, no. 3, pp. 1771–1781, 2016.

[25] P. Clifford, "Preliminary Sketch of Biquaternions," *Proceedings of the London Mathematical Society*, vol. 4, pp. 381–395, 1871/73.

[26] Z. Ji, H. Lin, and H. Yu, "Leaders in multi-agent controllability under consensus algorithm and tree topology," *Systems & Control Letters*, vol. 61, no. 9, pp. 918–925, 2012.

[27] V. Brodsky and M. Shoham, "Dual numbers representation of rigid body dynamics," *Mechanism and Machine Theory*, vol. 34, no. 5, pp. 693–718, 1999.

[28] X. Wang, D. Han, C. Yu, and Z. Zheng, "The geometric structure of unit dual quaternion with application in kinematic control," *Journal of Mathematical Analysis and Applications*, vol. 389, no. 2, pp. 1352–1364, 2012.